Fatigue crack growth in heat-affected zone of butt-welded AISI 316 steam pipes

R. CUSOLITO and V. MANDORINI, Istituto Ricerche Breda, Milan, Italy.
D. D'ANGELO, Centro di Ricerca Termica e Nucleare, ENEL, Milan, Italy.

Abstract
The aim of this paper is to report the methodology and results of fatigue crack propagation tests at high temperature on an actual TP 316 H stainless steel heat-affected zone. Some metallographical investigations are also reported linking the effect of local microstructures with the variable crack propagation rate.
Finally, the residual life assessment of a cracked steampipe is briefly analysed as a typical application of the Fracture Mechanics approach at high temperature to check the structural stability of power plant components.

Riassunto
Propagazione di cricche per fatica nella zona termicamente alterata di saldature di testa di tubazioni vapore in AISI 316
Scopo del lavoro è presentare la metodologia ed i risultati di prove di propagazione di cricche per fatica ad alta temperatura nella zona termicamente alterata di un giunto prelevato da una tubazione in acciaio inossidabile AISI TP 316 H.
Sono riportate anche alcune indagini metallografiche al fine di collegare l'effetto della microstruttura locale con le variazioni della velocità di propagazione della cricca.
I dati ottenuti sono stati infine utilizzati per una stima approssimativa della vita residua di una tubazione esercita ad alta temperatura, mediante approcci basati sulla Meccanica della Frattura.

Introduction

The design of electric power plant components and the residual life assessment of high-temperature serviced materials are generally based on their mechanical and creep characteristics. This approach provides a satisfactory knowledge of the bulk material behaviour under uniform stress fields and, focusing attention on the steam pipeline, its fitness for purpose can be demonstrated by means of creep-rupture post-exposure tests on the base materials.
However, in singularities, particularly in welded zones, where the total stress is high and the microstructure features poor, crack-like defects can develop, as confirmed by non-destructive inspection performed periodically in the power plant, and grow subcritically during operation. Therefore, the in-service stability assessment of such weldments, strictly connected with safety and reliability issues, makes it necessary to consider both the accumulation of creep damage as a microstructure degradation in the homogeneous regions of the parent material, and the creep cavitation leading to cracking in the weld metal, as well as in the heat-affected zone.
During start-up, shut-down and electric load changes, a consistent increase in local stress was experienced, both theoretically by computer-assisted stress analysis and experimentally by on-line monitoring with capacitance strain-gauges, in the TP 316 H stainless steel steam pipe of a 660 MWe supercritical-pressure thermal power plant with an operation time of about 80,000 hours. The extensive circumferential cracking, located in the heat-affected zone, was demonstrated to be mainly due to the contemporaneous local presence of high variable stresses originated from constrained thermal expansion and to coarse-grain fully solubilized austenitic microstructure. The Fracture Mechanics approach allows in-service tolerance of such defects to be assessed, correlating the applied stress intensity factor with the fatigue-crack propagation rate at operation temperature. The aim of this paper is thus to report the methodology and results of fatigue crack propagation tests at high temperature on an actual TP 316 H stainless steel heat-affected zone. Some metallographical investigations are also reported, linking the effect of local microstructures with the variable crack-propagation rate.
Finally, the residual life assessment of a cracked steam pipe is briefly analysed as a typical application of the Fracture Mechanics approach at high temperature to check the structural stability of power plant components.

Material

The investigated material was cut out, after about 80,000 h operation, from the main steam piping in AISI 316 H stainless steel of a 660 MWe power plant with a supercritical cycle of 540°C as operation temperature, and 25 MPa as steam pressure.
The pipe testpiece was placed near the high-pressure turbine inlet, with 275 mm diameter, 40 mm wall thickness and 73 MPa hoop stress due to steam pressure.
The chemical composition, together with the ASTM A 376 TP 316 H code requirements, are reported in Table 1 showing full compliance with the prescribed element percentages.
The multipass circumferential butt weld, as shown in Figure 1, consists of weld beads deposited with electrodes after the groove initial closure made by means of the tungsten inert-gas technique. Also included in Figure 1 are typical hardness results of the

TABLE 1 - Chemical composition (wt %)

	C	Mn	Si	P	S	Cr	Ni	Mo
Serviced steel	.069	1.71	.46	.012	.012	16.46	13.78	2.24
A 376 Tp 316 H	.04 – .10	2.00 max	.75 max	.040 max	.030 max	16.0 – 18.0	11.0 – 14.0	2.00 – 3.00

Fig. 1 - Microstructure of the cross section of the 316 H pipe weldment and location of the drawn specimens.

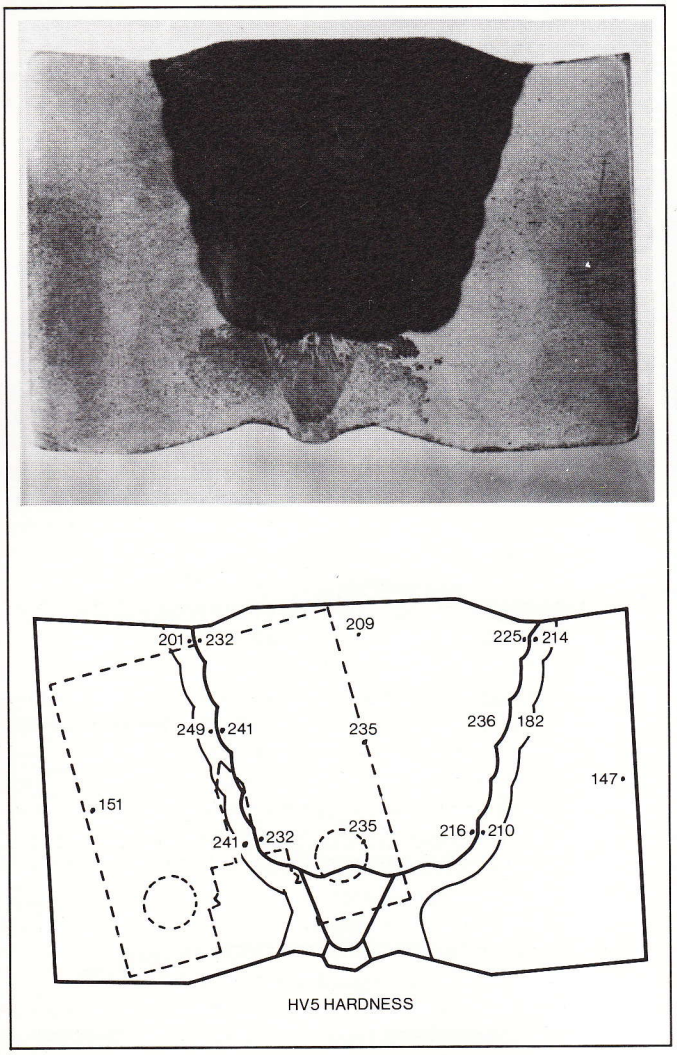

Fig. 2 - Microstructure features of the 316 H cross section butt weldment.

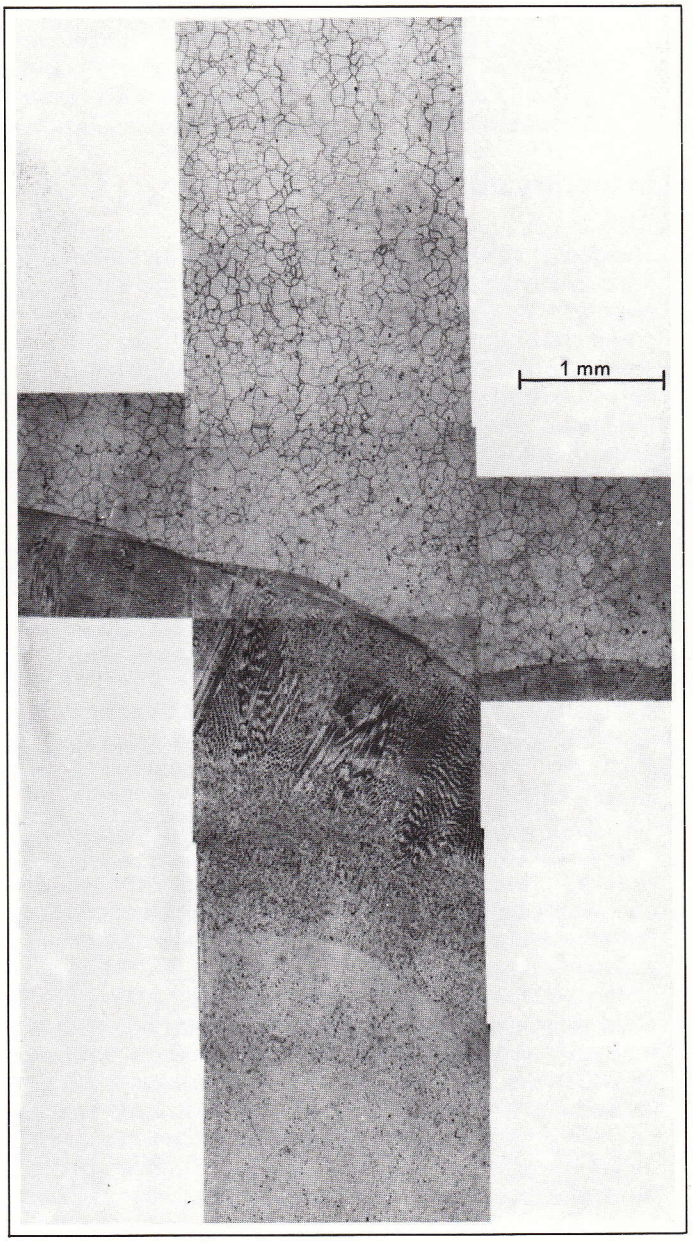

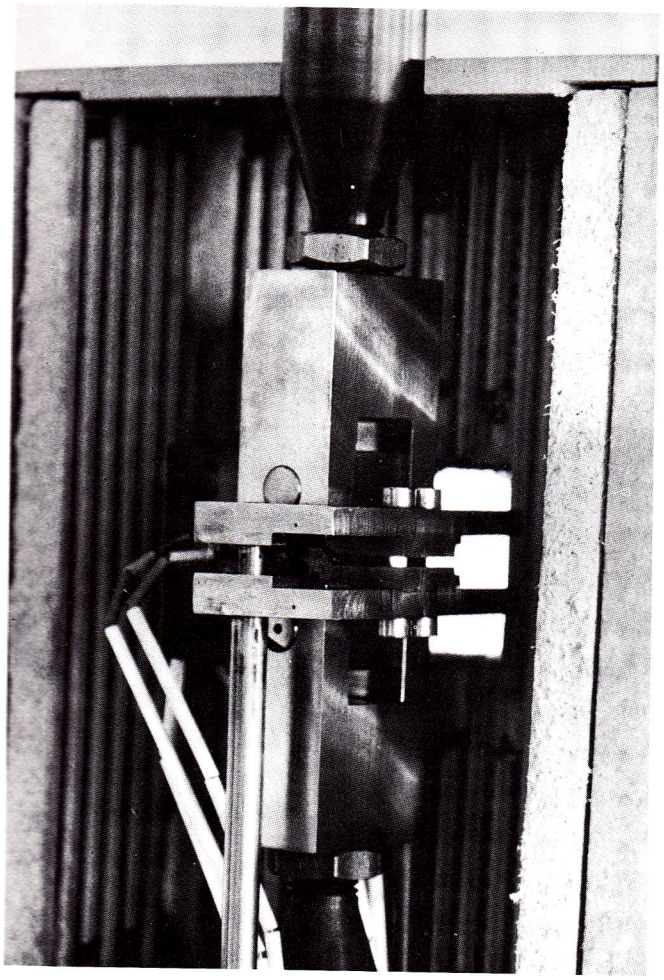

Fig. 3 - Detail of the instrumented specimen with related extensometer inside the oven.

weld cross section; the high values in the heat-affected zone indicate that some relevant plastic deformation has occurred in that thin area during pipe operation. The microstructures of the weld transverse cross section, Figure 2, particularly refer to the weld metal and to the heat-affected zone, where columnar and coarse grain structures are respectively exhibited. Computer-assisted analyses of pipe flexibility and of sectional stresses have been made[1] for typical transients, such as cold and hot start-ups. The maximum axial stresses due to pressure and temperature, on the external pipe fibre were calculated, their values ranging from 44 MPa to 59 MPa. The variable stress originating from constrained thermal expansion had a maximum axial value of 69 MPa. Finally, even after such prolonged power-plant operation, it can be assumed[2] that in the heat-affected zone an axial residual stress of about 100 MPa due to the welding process continues to act.

Experimental

Five fatigue tests were made, utilizing standard CT 1/2" specimens, drawn from the pipe as shown in Figure 1. The notch was always positioned along the HAZ of the circumferential welded joint. Fatigue tests were conducted at 550°C, on an Instron model 1362 electromechanical machine, on load control, with 1 Hz triangular waveform and stress ratio R = 0.05. Three of them were of pure fatigue and two had a maximum load level hold time of 10 minutes.
In Table 2 the load levels and the initial values of the stress intensity factor range for all the tests are reported.
The instantaneous crack length was measured by a method set up previously.[3] Briefly, during the test the load-notch opening curves were periodically recorded and, from these, the elastic compliance was evaluated.

TABLE 2 - Test data and results on fatigue crack propagation

Specimen No.	Frequency Hz	Hold-time min	Load levels Pmin N	Load levels Pmax N	ΔK_{in} MPa·m$^{\frac{1}{2}}$	N_f cycle	Paris law parameters (*) Co	Paris law parameters (*) m
1	1	0	259	5177	26.1	8445	1.68×10^{-10}	3.17
2	1	0	156	3110	16.8	24871	3.1×10^{-11}	3.54
3	1	0	207	4140	24.9	7006	1.58×10^{-12}	4.12
5H	—	10	207	4140	20.0	5655	3.22×10^{-17}	6.67
6H	—	10	259	5177	28.6	1824	2.12×10^{-17}	6.79

(*) for da/dN in m/cycle and ΔK_I in MPa·m$^{\frac{1}{2}}$

TABLE 3 - Specimen No. 2 (ΔK_{in} = 16.8 MPa·m$^{1/2}$, HT = 0)
Results of the "Incremental Polynomial method"

SAMPLE # ENEL M 2

CYCLES	A (MIS) mm	A (REG) mm	DA/DN mm/cycle	DS kgf/mm^2	DK kgf/mm$^{3/2}$
11400	15.637	15.644	.1194E-03	32.999	68.251
11600	15.673	15.664	.1141E-03	33.151	68.482
12000	15.703	15.710	.1151E-03	33.487	68.990
12200	15.739	15.733	.1279E-03	33.659	69.251
12400	15.754	15.757	.1566E-03	33.836	69.518
12600	15.783	15.787	.1649E-03	34.068	69.868
12700	15.790	15.808	.1575E-03	34.223	70.100
12800	15.828	15.823	.1624E-03	34.343	70.282
13000	15.880	15.860	.1732E-03	34.628	70.710
13200	15.895	15.897	.1661E-03	34.916	71.144
13400	15.909	15.928	.1507E-03	35.163	71.514
13600	15.962	15.952	.1379E-03	35.354	71.800
13800	15.985	15.976	.1350E-03	35.547	72.088
14000	16.000	16.004	.1423E-03	35.777	72.432
14200	16.024	16.034	.1424E-03	36.021	72.797
14400	16.062	16.061	.1343E-03	36.242	73.126
14600	16.093	16.092	.1365E-03	36.501	73.513
15000	16.155	16.148	.1290E-03	36.972	74.212
15200	16.171	16.173	.1250E-03	37.187	74.531
15400	16.195	16.194	.1306E-03	37.367	74.799
15600	16.210	16.218	.1314E-03	37.584	75.120
15800	16.242	16.240	.1382E-03	37.777	75.406
16000	16.265	16.270	.1539E-03	38.036	75.788
16200	16.313	16.304	.1601E-03	38.347	76.248
16400	16.330	16.340	.1676E-03	38.667	76.719
16600	16.377	16.375	.1661E-03	38.989	77.193
16800	16.418	16.409	.1649E-03	39.307	77.660
17000	16.435	16.433	.1760E-03	39.531	77.989

The opening was measured with a suitable spring-fitted mechanical extensometer which drove two LVDT's external to the oven. Figure 3 shows a view of the specimen and the mounted extensometer. The crack length was also optically observed by means of two travelling microscopes.
In order to obtain the crack rate da/dN vs ΔK curves, the analogically sampled test data were worked out off-line by a computer programme derived from the "Incremental Polynomial method" recommended by the ASTM E 647 code.
As an example, Table 3 gives the data concerning specimen No.2. In the columns, in the order, are shown: the cycle number, crack length as deduced by the compliance (a < mis >), its value as obtained by the n-points best-fitting curve (a < reg >), crack rate da/dN, stress and stress intensity factor range for the fatigue cycle.

Test results and analysis on fatigue crack growth

In Figure 4 the a-N curves for all the tests are reported. As one can see, some curves have a "wavy" behaviour: in other words, they present some zones at increasing and others at decreasing slopes.
This is ascribable to crack propagation direction changes which occur whenever the crack, strictly following the heat-affected zone (HAZ), crosses geometrical or toughness variation zones of the HAZ, produced by subsequent passes in the weld bead. See, for example, the macrography of the No. 3 specimen lateral face, shown in Figure 5a, and compare the crack path shown there with the corresponding a-N curve plotted in Figure 4: the agreement is fairly good.
Crack propagation direction is, however, not constant in the specimen thickness, due probably to both the high

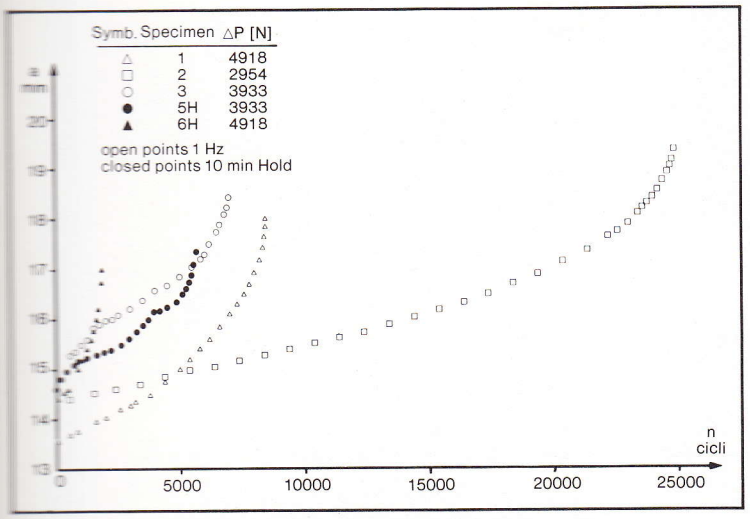

Fig. 4 - Crack length versus number of cycle curves for all specimens.

residual stresses and to the different conformations of subsequent passes in the weld bead.
In Figure 5b one can namely notice that, on the opposite side of the same No. 3 specimen, fatigue crack propagation runs completely in the fused zone. In spite of crack propagation discontinuities, all the da/dN vs ΔK curves on log-log coordinates always present a rectilinear segment, as can be ascertained from Figure 6, relevant to specimen No. 5H.
Hence it was possible to specify, for every specimen, a stress-intensity factor range interval where the Paris relationship is valid

$$\frac{da}{dN} = C_o (\Delta K)^m$$

The C_o and m best-fitted values are given in Table 2, while all the crack propagation curves are plotted in Figure 7. As one can see from this, the tests with hold-time yielded a crack propagation rate higher than those without hold-time, the difference increasing with the increase of applied ΔK_I.
The values obtained for crack rate agree fairly well with the small amount of data given in the literature.[4]
It should be underlined, in any case, that the overall behaviour of the da/dN vs ΔK function is a very complex one, and care should be taken when extracting data from such a function.
In Figures 8-9 SEM micrographs are shown of the No. 1 and No. 6H specimen fracture surfaces. Both had been subjected to the same load: the former without and the latter with a 10 min hold-time. In Figure 8a we can see an inter-transgranular mixed mode crack propagation,

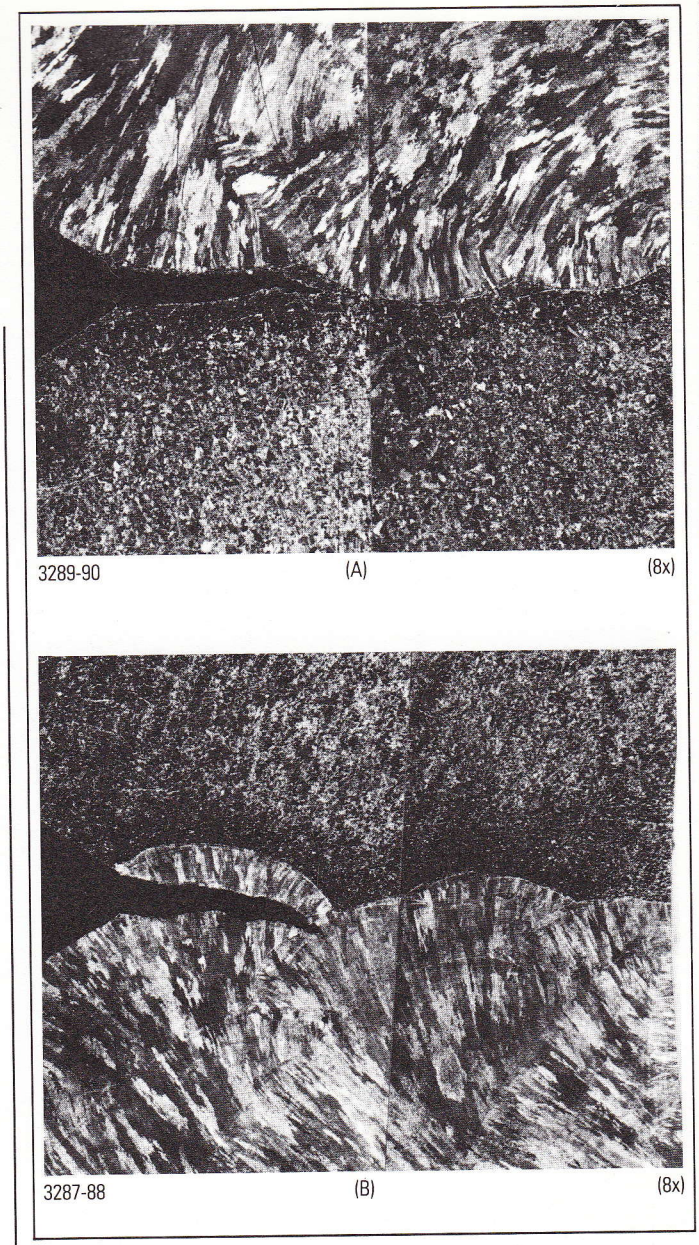

Fig. 5 - Crack propagation path on both sides of the specimen No. 3.

Fig. 6 - Crack growth rate behaviour for the specimen 5H (ΔK_{init} = 20 MPa $\sqrt{m}$, H.T. = 10 min)

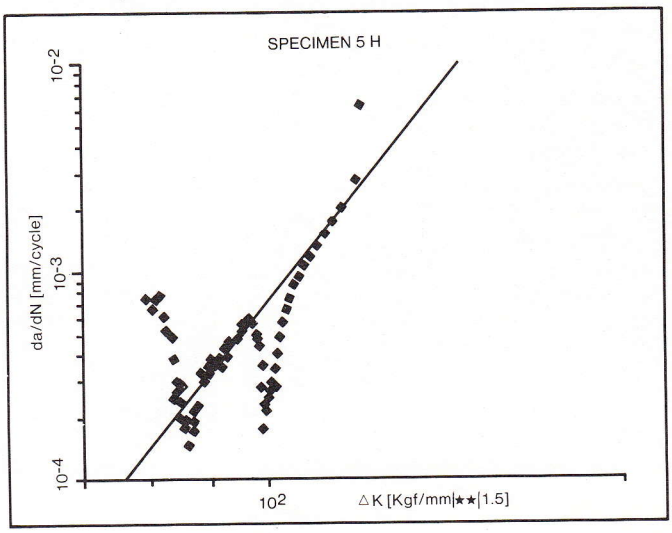

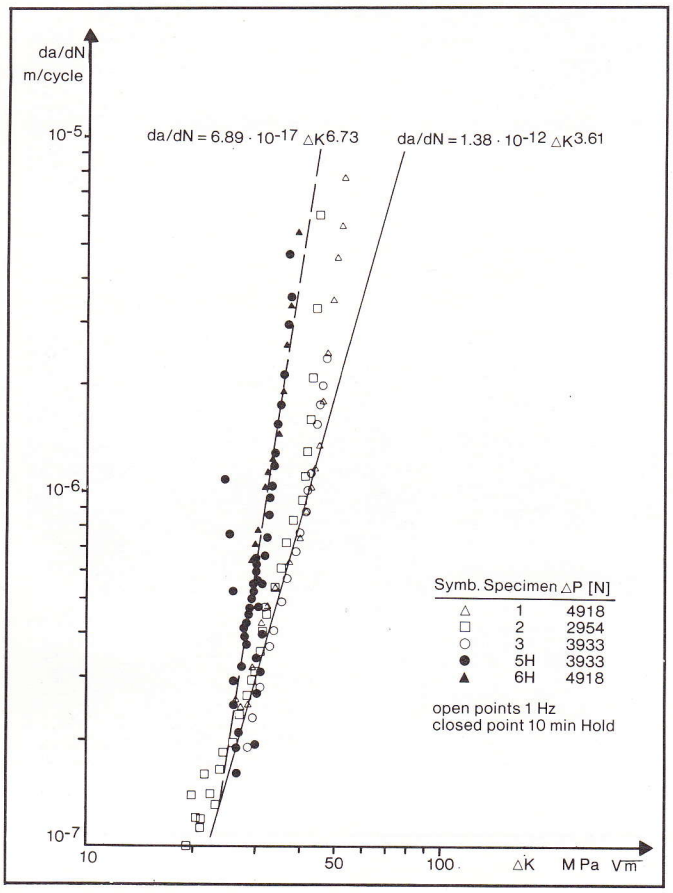

Fig. 7 - Crack growth rate behaviour for all specimens.

Fig. 8 - SEM micrographs of specimen No. 1 (ΔK_{init} = 26.1 MPa $\sqrt{m}$ – H.T. = 0).

which at higher magnification reveals limited striation-affected zones (see Figure 8b). At the notch apex, corresponding to the last phases of crack propagation, a ductile fracture by microvoid coalescence is present, in accordance with the findings of other authors[5] (see Figure 8c).
For the 6H specimen (tested with hold-time, see Figure 9a), fatigue striations disappear and the intergranular cavitation fracture mechanism (see Figure 9b) predominates.

Fatigue life assessment

The fatigue crack propagation data obtained from the tested specimens were utilized for a first-approach estimate of steam pipe fatigue life in the service conditions given at the beginning.
Flaws detected on such components generally originate inside the pipe wall, close to the outside surface, in the HAZ of circumferential welded joints. They then grow, partly emerging to the outside surface, partly lengthening along the pipe periphery, until they embrace the whole circumference.
Owing to the presence of strong compressive residual stresses on the inside surface, the flaws never become through-the-thickness ones.
Consequently, the hypothesized pipe-damage mechanism refers to a circumferential surface crack, which, under the action of a uniform axial tensile stress field, grows only lengthwise and not in depth.
Moreover, owing to high steel toughness, it is very

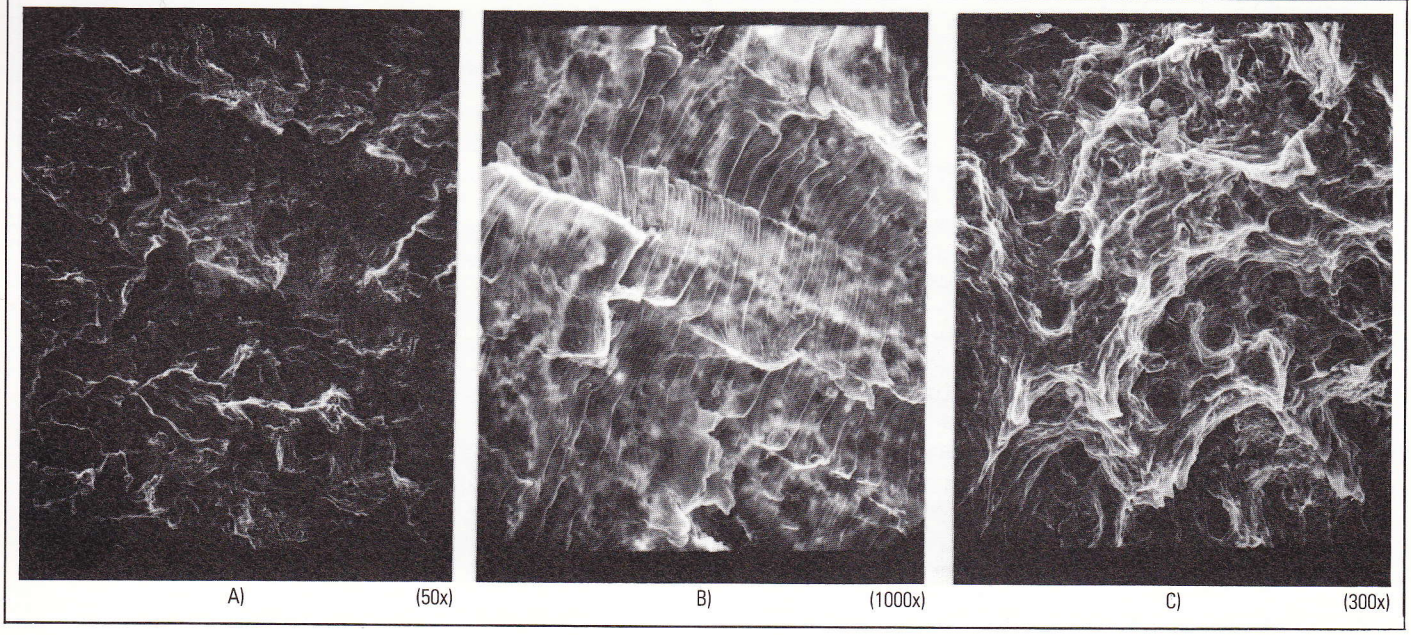

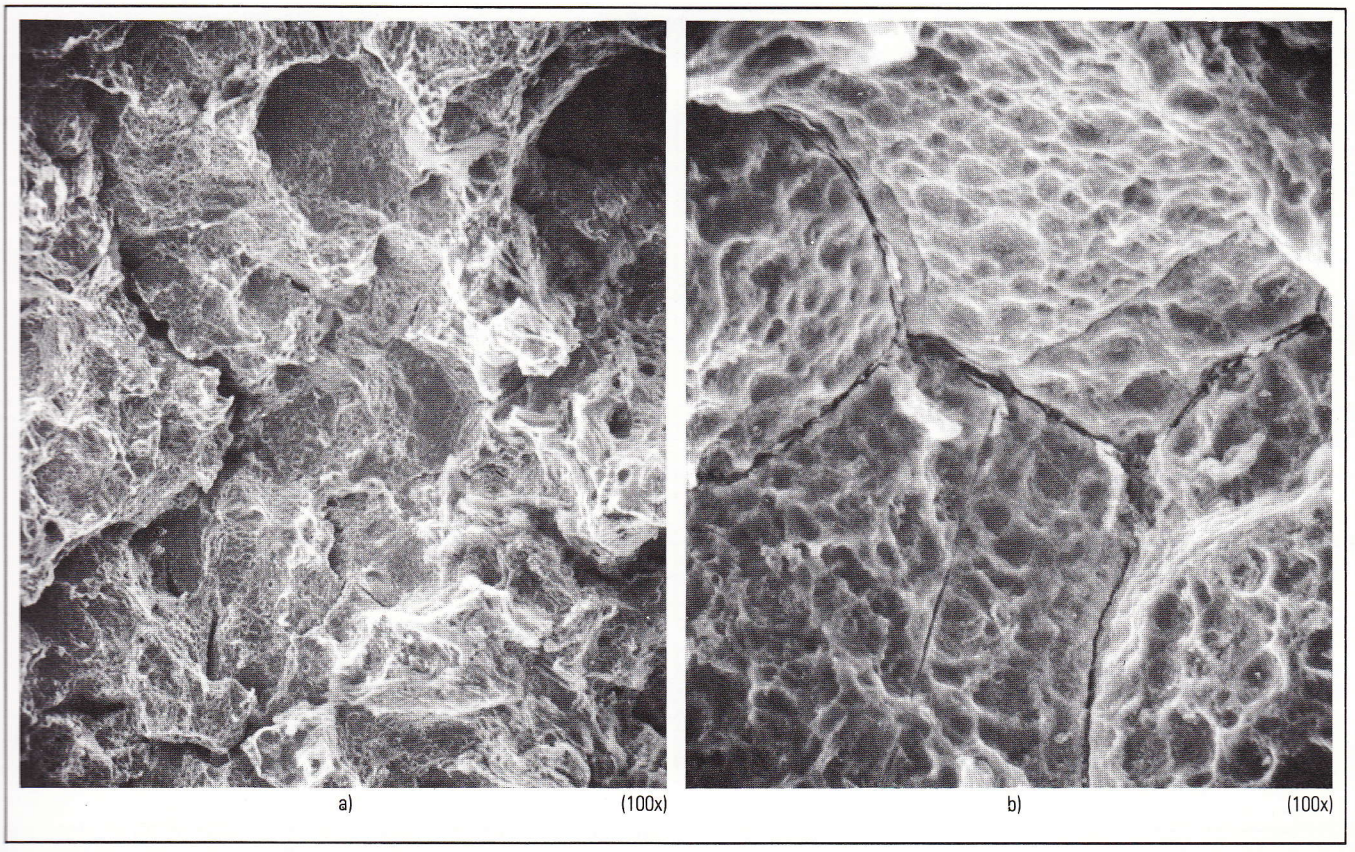

Fig. 9 - SEM micrographs of the 6H specimen (ΔK_{init} = 28.6 MPa $\sqrt{m}$ — H.T. = 10 min).

unlikely that an unstable fracture will occurre into the pipe, before the crack has involved the whole periphery, as was demonstrated by Tada and Paris through a fully-plastic analysis of BWR-AISI 304 steel nuclear steam pipes.[6]

Presumably, only after the crack has covered the whole periphery it begins to deepen, finally leading to pipe collapse.

Conservatively, pipe ultimate life has been assumed to coincide with the fatigue cycle number necessary to the crack for describing the whole circumference.

For the geometry under study there is no K_I-solution: approximate formulations have therefore been adopted, which nevertheless reflect the phenomenon physics and result, in any case, conservative. The checked solutions are as follows:

1 - As zero-order approximation, the flaw was considered as a through-the-thickness one. Hence the stress-intensity factor is given by the Folias equation:[7]

$$K_I^{(\circ)} = \left\{ \frac{8\bar{\sigma}c}{\pi} \ln \sec \left(\frac{\pi M \sigma}{2\bar{\sigma}} \right) \right\}^{1/2} \qquad (1)$$

where c is the flaw half-length, M is the surface curvature correction factor and $\bar{\sigma}$ is the flow-stress.

2 - As first-order approximation, the geometry under examination was assumed to be like a flat plate containing a surface flaw. The relevant K_I' is given by an equation proposed by Newman and Raju,[8] modified by M for curvature effects, which can be put in the form:

$$K_I' = M\sigma \left(\frac{a}{Q} \right)^{1/2} F \left(\frac{a}{t}, \frac{a}{c}, \frac{c}{w}, \Phi \right) \qquad (2)$$

where a, c, t, w, ø have the meaning as shown in Figure 10, Q is a function of a/c and F is a cumbersome function of the indicated variables.

3 - As a further first-order approximation, a K_I'' was developed, following the outlines of Dawes methodology for surface defects,[9] which has been adopted by IIW in the C.O.D. design curve. The surface flaw in a flat plate was substituted, in said methodology, by an " equivalent " through flaw, a flaw which, in other terms, has, under the same

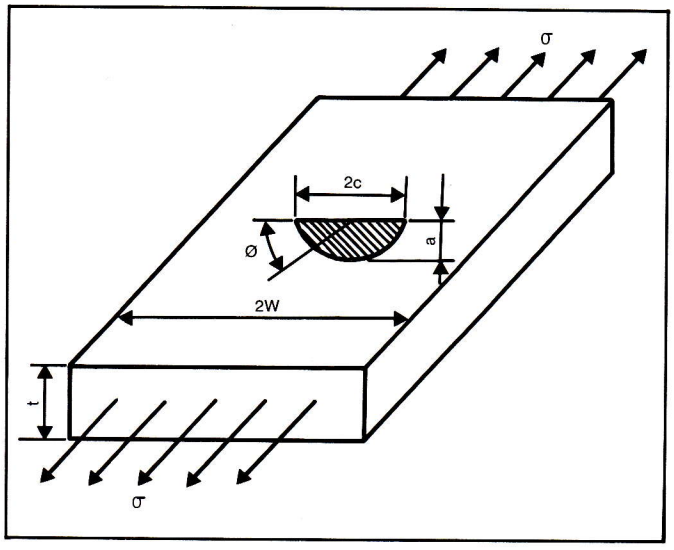

Fig. 10 - Typical parameters of flat plate surface crack.

Fig. 11 - Fatigue life of the pipe by different approximations.

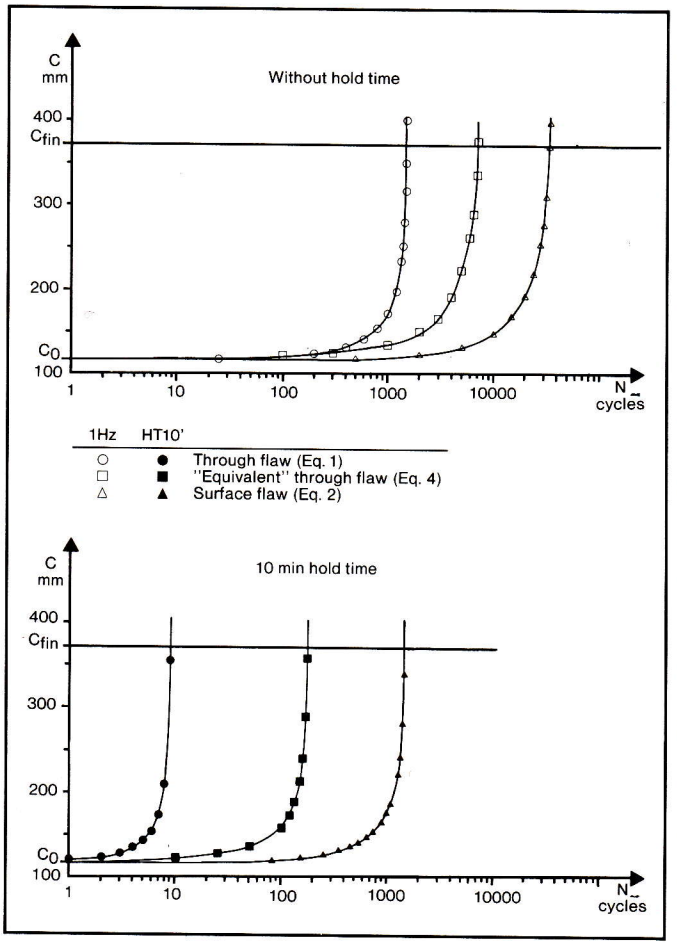

applied load, the same stress intensity factor.
The equivalent flaw half-length can be obtained by eq (2) (without M) with little algebra as

$$C_{eq} = \frac{a}{Q} F^2 \left(\frac{a}{t}, \frac{a}{c}, \frac{c}{w}, \Phi\right) \quad (3)$$

and the relevant K_I is given by eq (1) with $C = C_{eq}$:

$$K''_I = K_I^{(\circ)} (C_{eq}) \quad (4)$$

Two flaws were taken into consideration. They represent somewhat limiting cases for this type of flaw. Their sizes are as follows

Flaw	a mm	c mm	a/c	a/t
A	25.0	117.5	0.21	0.60
B	1.3	6.5	0.20	0.03

As far as acting stresses are concerned, preliminarily only those due to internal pressure and to pipe constrained expansion during thermal transients were taken into account. This gives a stress σ of 127 MPa, which compared to an estimated value for the flow-stress $\bar{\sigma}^{(10)}$ of 347 MPa, yielded $\sigma/\bar{\sigma} = 0.36$. The computed results are given in Table 4 and, in graphical form, in Figure 11.
As one can see from the table, for the larger flaw (A) the approximation (3) of the " equivalent " flaw yields results which are intermediate between those relevant to the through and the surface flaw solutions; it is reasonable therefore to think that the attempted estimate is quite realistic.
For the smaller flaw (B) the two first-order K_I approximations resulted lower than the ΔK_{in} of the fatigue tests: this prevented residual life estimation. There are however some grounds for thinking that, for very small flaws, the most suitable approximation is formulation (2) relevant to flat plate, corrected for surface curvature.
In any case the examined solutions should be considered as a preliminary screening, awaiting more rigorous approaches.
Another result emerging from Table 4 is the hold-time influence on fatigue life: even with a hold-time of only 10 min at maximum load, fatigue life reduction is very high, in the range of 10^2–10^3.

Conclusions

The study presents a contribution to the fatigue life assessment of power plant stainless steel steam pipes which suffer cracking in the HAZ of circumferential welded joints.

TABLE 4 - Residual life computation results

Approximation	Flaw type			
	A (a = 25 mm, c = 117.5 mm)		B (a = 1.3 mm, c = 6.5 mm)	
	Fatigue life, N_f			
	HT = 0	HT = 10 min	HT = 0	HT = 10 min
1 - Through flaw (Eq. 1)	1535	10	130000	109000
2 - Surface flaw (Eq. 2)	34000	1510	—	—
3 - " Equivalent " through flaw (Eq. 4)	7200	175	—	—

The assessment was based on fatigue test results and a Fracture Mechanics approach.
Fatigue tests demonstrated that, without hold-time, crack growth ranged between 10^{-7} and 10^{-6} m/c, varying the applied ΔK_I from 20 to 40 MPa $m^{\frac{1}{2}}$.
Hold-time increases the rate by at least one order. This is due to deeper contribution to crack propagation, coming from the creep damage mechanism, as was demonstrated by the SEM analysis of fracture surfaces.
In order to assess pipe fatigue residual life, two approximate solutions were tested for the K_I relevant to the examined surface flaws. It was ascertained that the definition of an " equivalent " flaw, in the sense given by IIW, yields, at least for not too small flaws, quite reasonable results.
However, much work remains to be done, in order to arrive at a precise definition of pipe life.
Actions to be carried out could be summarized as follows:

1 - Acquisition of much more data for the propagation morphology of flaws in the HAZ;
2 - Deepening of hold-times and P effect knowledge on the crack propagation rate and of the way these parameters affect creep-fatigue interaction micromechanisms;
3 - More rigorous definition of the K_I-solutions for circumferential surface flaws.

Acknowledgments

The work was supported by ENEL-CRTN, which is greatly acknowledged. Thanks are also due to Miss P. Bianchi of CRTN, who performed the S.E.M. analysis.

REFERENCES

(1) Cesari, F., S. Ghia, A. Macchi, V. Regis, and S. Menghini. Theoretical and experimental analysis of steam piping for supercritical power plant. ***6th Conf. on "Structural Mechanics in Reactor Technology",*** *Paris, France, 17-21 August 1981.*

(2) Darbyshire, J.M., J.K.L. Lai, and B. Nath. Metallographic examination and residual stress measurements of type 316 weld metals. ***CEGB-CERL Rep. No RD/L/N 105/80,*** *September 1980.*

(3) Mandorini, V., R. Cusolito, and C. Colombo. Experimental methodologies in the high temperature fatigue crack-growth analysis. ***11th National Congress of AIAS,*** *Torino, Italy, 26-28 Sept. 1983, 55-68 (in Italian).*

(4) Lloyd, G.J., and J.D. Walls. Propagation of fatigue cracks from surface flaws in austenitic type 316 butt welds. ***Eng. Fract. Mech., 13*** *(1980), 897-911.*

(5) Pickard, A.C., R.O. Ritchie, and J.F. Knott. Fatigue Crack Propagation in a type 316 stainless steel weldment. ***Metals Technology,*** *June (1975), 253-263.*

(6) Tada, H., P.C. Paris, and R.M. Gamble. A stability analysis of circumferential cracks for reactor piping systems. ASTM ***STP 700*** *(1980), 296-313.*

(7) Folias, E.S. On the theory of fracture of curved sheets. ***Eng. Fract. Mech., 2*** *(1970), 151-164.*

(8) Newman, J.C., and I.S. Raju. An empirical stress-intensity factor equation for the surface crack. ***Eng. Fract. Mech., 15*** *(1981), 185-192.*

(9) Dawes, M.G. Fracture control in high yield strength weldments. ***Welding Jrnl, Res. Suppl., 53*** *(1974), 369-s.*

(10) Hawthorne, J.R., and B.H. Menke. Influence of delta ferrite on notch toughness of austenitic stainless steel weldments. ***ASME Symp. on "Structural Materials for service at elevated temperatures in Nuclear Power Generation".*** *Houston, Texas, Nov. 30th, 1975.*